

Fragmentation of C₆₀ and C₇₀ clusters

Eunja Kim and Young Hee Lee*

Department of Physics, Jeonbuk National University, Jeonju 560-756, Korea

Jae Young Lee

Department of Agricultural Engineering and Semiconductor Physics Research Center, Jeonbuk National University, Jeonju 560-756, Korea

(Received 7 June 1993)

We have investigated the fragmentation of C₆₀, C₇₀ carbon clusters using molecular-dynamics simulation combined with the empirical-tight-binding total-energy-calculation method. The fragmentation process is studied by considering the heat capacity, binding energy, and the average number of neighboring atoms in terms of temperature and the relation to the formation process is further discussed.

I. INTRODUCTION

An extensive study of carbon clusters has recently been carried out both experimentally and theoretically. These clusters have shown great potential for application in new materials since Krätschmer *et al.*¹ generated C₆₀ molecules from various fullerenes by chemical treatments.

One of the fundamental questions is the following: What is the formation mechanism of the special ball-like shapes of the various fullerenes? It is still difficult to clarify this question since there exist various experimental conditions which are not easy to control. A theoretical study of the nucleation process of C₆₀ has been done.² However, disordered C₆₀ has been obtained by slow quenching of random carbon clusters, implying that more complicated experimental situations are involved during the formation process. The fragmentation phenomenon is very interesting, and is related to the formation mechanism since this may give some clues for the formation process. Various fullerene structures are found from mass spectroscopic measurement. It will be, therefore, worth comparing the fragmentation phenomena of C₆₀ with that of C₇₀.³

It is difficult to treat theoretically the melting phenomena of many-electron systems. We adopt a molecular-dynamics (MD) simulation combined with the empirical-tight-binding (TB) method for electronic band-structure calculation. The validity of this scheme is, therefore, the correct choice for empirical tight-binding parameters. Recently, Wang *et al.*⁴ have determined these parameters for the carbon system which can reproduce the universal binding energy curves of various phases from first-principles calculations. This potential has been successfully applied to many different systems.

II. THEORY

In the TB MD scheme, the total Hamiltonian is rewritten as

$$E = \sum_I \frac{P_I^2}{2m} + \sum_n^{\text{occupied}} \langle \psi_n | H_{\text{TB}} | \psi_n \rangle + U_{\text{rep}}. \quad (2.1)$$

The first term is the kinetic energy of atoms, and the second term is the electronic energy calculated from a parametrized tight-binding Hamiltonian H_{TB} . The orthogonal sp^3 basis involves the following parameters: ε_s and ε_p are on-site s and p energy levels, respectively, and $v_{ss\sigma}$, $v_{sp\sigma}$, $v_{pp\sigma}$, and $v_{pp\pi}$ are overlap integral parameters as a function of separated distance. The third term is a short-range repulsive energy in the form of $U_{\text{rep}} = \sum_{I < J} f[\sum_J \phi(r_{IJ})]$ where $\phi(r_{IJ})$ is the pairwise potential function. The above parameters and functions were fitted to first-principles calculation results of electronic band structure and binding energies from various crystalline carbon phases. Details of this method have been described elsewhere.⁴

Once the total energy calculational scheme is constructed via the TB method, the next step of TB MD is to calculate the forces on each atom. This can be achieved by taking the derivative of the total energy with respect to each atom, i.e.,

$$\mathbf{F}_i = m\mathbf{a}_i = -\frac{\partial E_{\text{tot}}}{\partial \mathbf{r}_i} = -\sum_n^{\text{occupied}} \left\langle \psi_n \left| \frac{\partial H_{\text{TB}}}{\partial \mathbf{r}_i} \right| \psi_n \right\rangle - \sum_{I < J} \frac{\partial U(r_{IJ})}{\partial \mathbf{r}_i}, \quad (2.2)$$

where the first term is called the Hellmann-Feynman force, and the second term comes from the repulsive pairwise potential. These forces are supplied to molecular-dynamics simulation and $3N$ -coupled second-order differential equations are solved numerically via the Gear algorithm.⁵ Because this method utilizes valence electrons of atoms only (in this case four electrons per atom), its efficiency is greatly enhanced compared to *ab initio* calculation, which is a very crucial factor for practical dynamical calculation. Thus, with choices of minimal

basis electrons both the efficiency and the accuracy are achieved.⁶

The band structure energy of each cluster is calculated at the Γ point. The time step 7.08×10^{-16} s is used. The total energy is conserved in 10^{-3} eV in the microcanonical ensemble energy surface at room temperature.

III. RESULTS AND DISCUSSION

C_{60} is constructed by cutting 12 vertices of an icosahedron. C_{70} is constructed by inserting 10 more atoms in the equator of C_{60} . These configurations may not be the equilibrium structures with our potentials. The TB MD simulation was performed for a few thousand time steps to equilibrate. The system was run again for 1500 time steps at a given temperature with a typical temperature control method and run for 1000 time steps in the microcanonical ensemble. Then the equilibrium structures, such as heat capacity, pair-correlation function, binding energy, and the number of neighboring atoms, are calculated by averaging over 1000 time steps.

Figure 1 shows the pair-correlation function of C_{60} and C_{70} at various temperatures. At ground states, two sharp peaks at 1.39 Å and 1.44 Å are observed, which is characteristic of single and double bonds of C_{60} whereas C_{70}

shows many intermediate bonds. However, the distinction in the first peak becomes obscure at 500 K due to the lattice vibrations. The distinction between the second and the third peak becomes blurred around 1500 K for both C_{60} and C_{70} . Around 4000 K one can clearly see the third peak disappear and the first and the second peaks start merging for both clusters. This indicates that the cage structures have changed.

Shown in Fig. 2 are the heat capacity and the binding energy of C_{60} and C_{70} as a function of temperature. At low temperature the values of heat capacity is very low (this is not shown in the figure). This becomes maximum around 3000 K and decreases with further increase of temperature and saturates at some constant values around 5000 K for both cases. Similar temperature dependence can be seen in the binding energy. The binding energy of C_{70} is a little greater than that of C_{60} . These values become lower as the temperature increases, due to the lattice vibration, and decrease sharply around 4000 K. This implies that the bond breaks around 4000 K. This analysis shows that both C_{60} and C_{70} reveal structural changes within the range between 3000 and 4000 K.

One can also count a number of neighboring atoms (Table I). Up to 3500 K the number of bonds are fixed

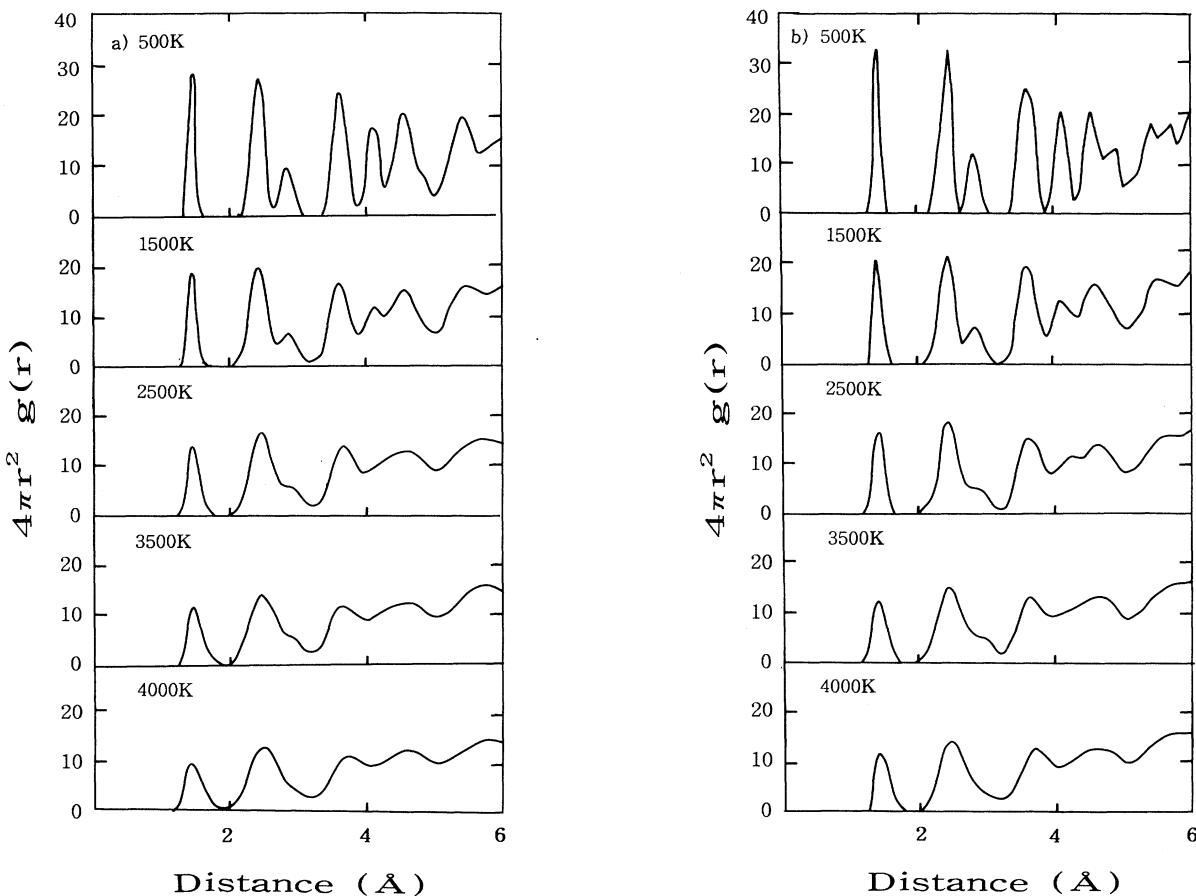


FIG. 1. The pair-correlation functions for various temperatures of (a) C_{60} and (b) C_{70} .

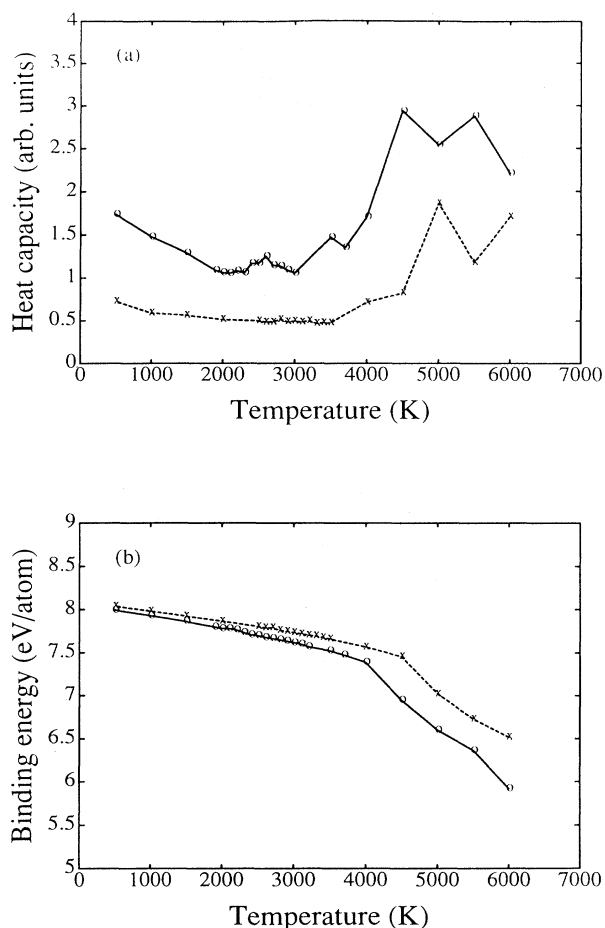


FIG. 2. The heat capacity and the binding energy as a function of temperature of C_{60} and C_{70} .

at three for both C_{60} and C_{70} , indicating complete cage structures. After 4000 K this number starts decreasing and eventually drops to 2.83 and 2.66 for C_{60} and C_{70} , respectively, around 5000 K.

Severe cage distortions are clearly illustrated in Fig. 3, which are the snapshots of C_{60} and C_{70} at 3000 K. Though the shapes of both clusters are severely distorted, they still maintain complete cage structures, as expected from the above analysis. The distortion ranges are 1.44 ± 0.39 Å. The bonds start breaking around 5000 K, as shown in Fig. 4. One notes that single bonds between a pentagon and a hexagon break first for C_{60} . Once the

TABLE I. Average number of nearest-neighbor atoms with the cutoff distance 2.0 Å in terms of temperature.

Temperature (K)	C_{60}	C_{70}
3000	3	3
3500	3	3
4000	2.93	2.94
4500	2.87	2.83
5000	2.83	2.66

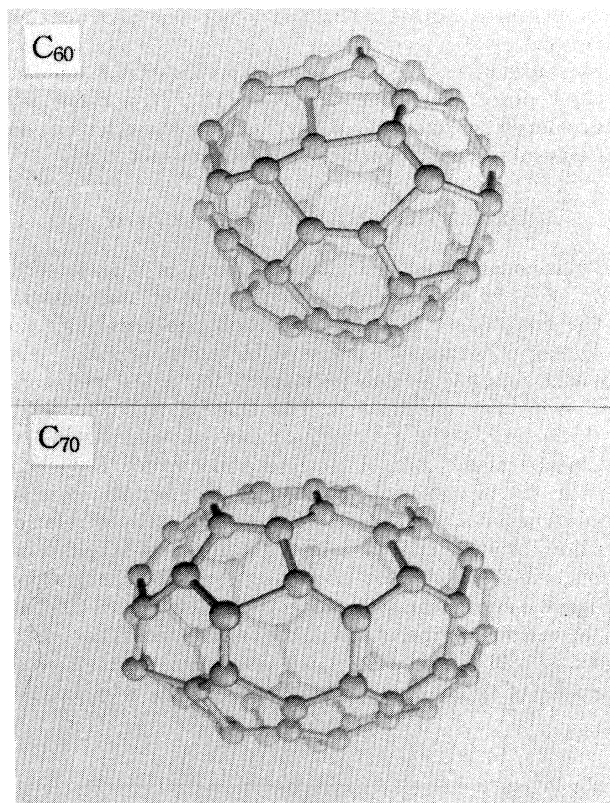


FIG. 3. Snapshots of C_{60} and C_{70} at 3000 K. Depth is identified by the brightness and the size of atoms. The brighter and the smaller the atom, the deeper the eyes. The bonds are artificial for views. We used 1.9 Å for the bond cutoff for the drawings.

single bond is broken, the stresses are accumulated near that bond, and the bond breakings are further developed to the neighboring bonds. This process occurs rapidly within one picosecond. One also sees that even the dimer can be formed during the fragmentation process. As time evolves, the C_{60} atoms are completely broken, forming linear chains. It has been suggested that with atoms $5 \leq n \leq 10$, the odd-numbered clusters prefer linear chain structures, whereas the even-numbered clusters prefer a ring structure.⁴ Similar behaviors are shown in C_{70} (see Fig. 5). The difference is that not only the single bonds between a pentagon and a hexagon but also single bonds between hexagons can be broken in C_{70} , contrary to the case of C_{60} . This is due to the fact that C_{70} has more single bonds near the equator than C_{60} does, which were introduced with an additional 10 atoms in the equator of C_{60} .⁷

We observe that dimer breaking also occurs in C_{70} . One can suggest that C_n clusters can be inserted when two C_{30} caps⁸ collide with each other during the formation process, making C_n clusters other than C_{60} . With this argument the yields of other clusters should be less than that of C_{60} , in good agreement with experimental observation. This conjecture can be proved by colliding C_{20} or C_{30} caps together with changing temperature of

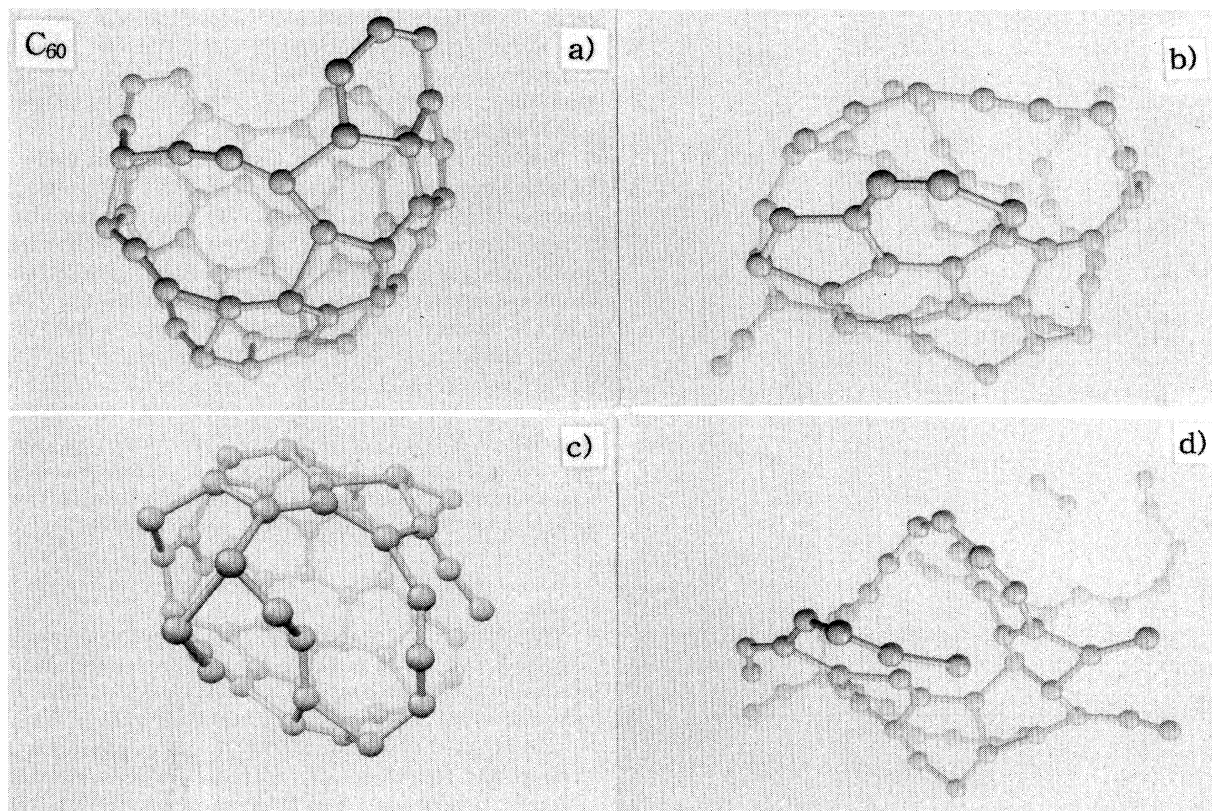


FIG. 4. Time evolution of snapshots of C_{60} at 5000 K for every 500 time steps.

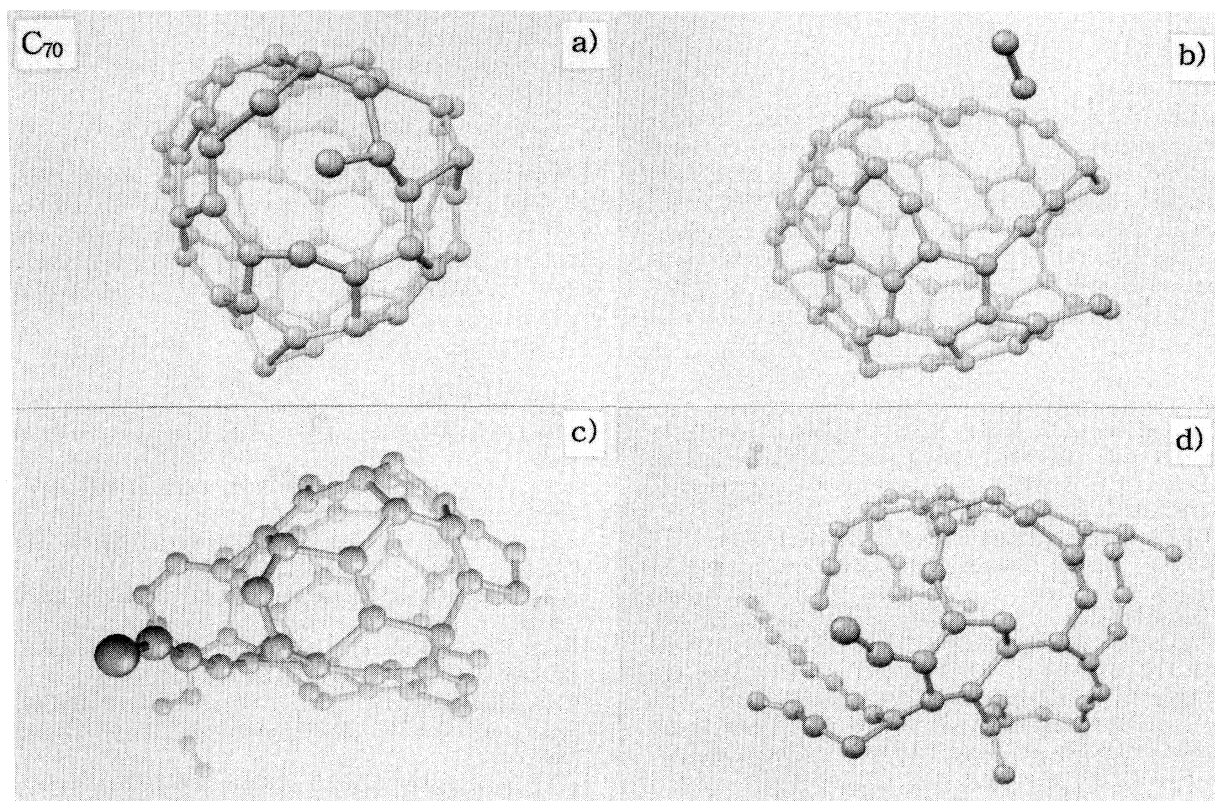


FIG. 5. Time evolution of snapshots of C_{70} at 5000 K for every 500 time steps.

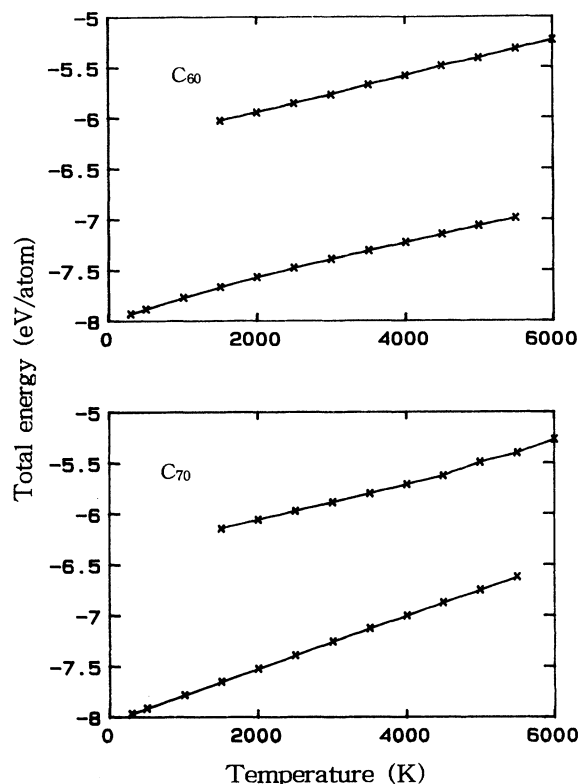


FIG. 6. The total energy as a function of temperature of C_{60} and C_{70} .

the clusters.

Figure 6 shows the total energy changes as a function of temperature. Starting from an ideal configuration for given temperature, one can get average values of the total energy. One can repeat this calculation from high temperature, i.e., above melting temperature. The latent heat, which is the energy difference at melting temperature, is 1.65 and 1.29 eV for C_{60} and C_{70} , respectively. We choose a melting temperature around 4000 K. (The melting temperature of diamond is 4100 K.) The latent

heat of graphite is 1.085 eV,⁹ experimentally. Since C_{70} has more hexagons near the equator, the electronic structures have more sp^2 -like orbitals than C_{60} . We expect, therefore, that this value gets closer to that of graphite with the large size of clusters.

It is interesting to note that bulk C_{60} in pellet form reveals structural changes around 700 °C to amorphous carbon.¹⁰ Park *et al.* (Ref. 11) also report that pyrolyzed pure C_{60} at 1000 °C for ten hours shows structural changes to amorphous materials. These observations are in contrast with our theoretical results that C_{60} and C_{70} form cage structures stably up to 3000 K. The characteristics of individual clusters might be different from those of the bulk. It is generally believed that the cage structures in the bulk interact via van der Waals forces and hence these interactions should not affect the temperature of structural changes. The severe lattice distortions may vary the structural changes in the bulk properties. This will be further investigated.

IV. SUMMARY

We have investigated the fragmentation process of C_{60} and C_{70} using a tight-binding molecular-dynamics method. The melting temperature of C_{60} and C_{70} is between 3000 and 4000 K, lower than that of diamond. Single bonds between a hexagon and a pentagon break first around 4000 K in C_{60} , whereas single bonds between not only a pentagon and a hexagon but also a hexagon and a hexagon break in C_{70} . A dimer molecule is formed during the fragmentation process in both C_{60} and C_{70} . Once the bonds start breaking, the fragmentation process occurs very rapidly, within a picosecond. The latent heats of C_{60} and C_{70} are 1.65 and 1.29 eV, respectively.

ACKNOWLEDGMENTS

We thank C. Z. Wang, K. M. Ho, and Y. W. Park for sending us their manuscript prior to publication. This work was supported by the Korea Science and Engineering Foundation (KOSEF) through Semiconductor Physics Research Center (SPRC) at Jeonbuk National University.

* Author to whom correspondence should be addressed.

¹W. Krätschmer, L. D. Lamb, K. Fostiropoulos, and D. R. Huffman, *Nature* **347**, 354 (1990); see also, H. W. Kroto, J. R. Heath, S. C. O'Brien, R. F. Curl, and R. E. Smalley, *ibid.* **318**, 162 (1985).

²J. R. Chelikowsky, *Phys. Rev. Lett.* **67**, 2970 (1991).

³H. W. Croto and K. McKay, *Nature* **331**, 328 (1988); R. E. Smalley, *Acc. Chem. Res.* **25**, 54 (1991); J. R. Heath, in *Fullerenes*, edited by G. S. Hammond and J. K. Valerie (American Chemical Society, Washington, D.C., 1992), Chap. 1; I. J. Ford and C. F. Clement, *Phys. Rev. Lett.* **69**, 387 (1992); D. H. Robertson, D. W. Brenner, and C. T. White, *J. Phys. Chem.* **96**, 6133 (1992); C. T. White *et al.*, in *Buckminsterfullerenes*, edited by W. E. Billups and M. A. Ciufolini (VCH, New York, 1993), Chap. 6.

⁴C. Z. Wang, C. H. Xu, C. T. Chan, and K. M. Ho, *J. Phys. Condens. Matter* **4**, 6047 (1992).

⁵C. W. Gear, *Numerical Initial Value Problems in Ordinary Differential Equations* (Prentice-Hall, Englewood Cliffs, NJ, 1971).

⁶C. Z. Wang, K. M. Ho, and C. T. Chan, *Phys. Rev. Lett.* **70**, 611 (1993).

⁷S. J. Woo, E. Kim, and Y. H. Lee, *Phys. Rev. B* **47**, 6721 (1993).

⁸R. A. Jishi and M. S. Dresselhaus, *Phys. Rev. B* **45**, 11305 (1992).

⁹*Lange's Handbook of Chemistry*, edited by J. A. Dean (McGraw-Hill, New York, 1985).

¹⁰C. S. Sundar, A. Bharathi, Y. Hariharan, J. Janski, V. S. Sastry, and T. S. Radhakrishnan, *Solid State Commun.* **84**, 823 (1992).

¹¹E. B. Park, J. W. Shim, H. J. Choi, and Y. W. Park, *Synth. Met.* **44**, 363 (1991).

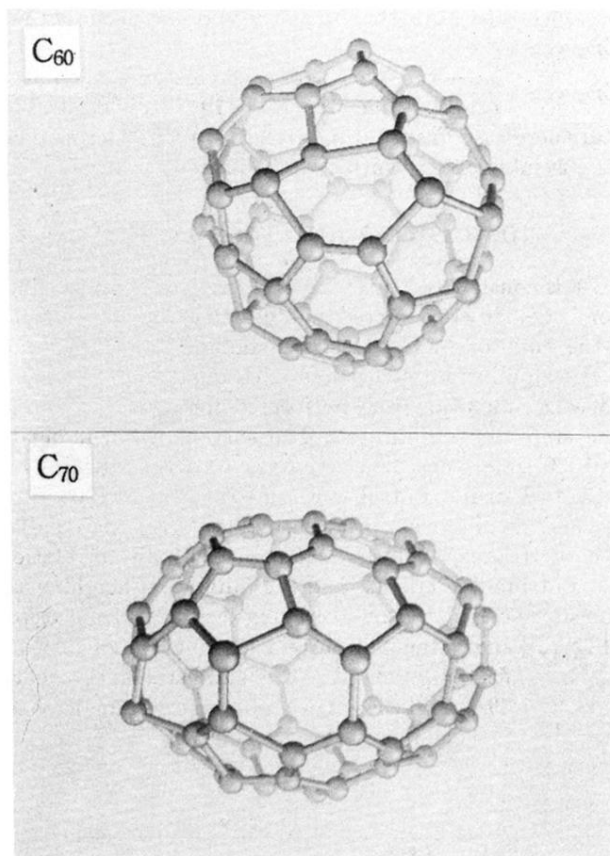


FIG. 3. Snapshots of C_{60} and C_{70} at 3000 K. Depth is identified by the brightness and the size of atoms. The brighter and the smaller the atom, the deeper the eyes. The bonds are artificial for views. We used 1.9 Å for the bond cutoff for the drawings.

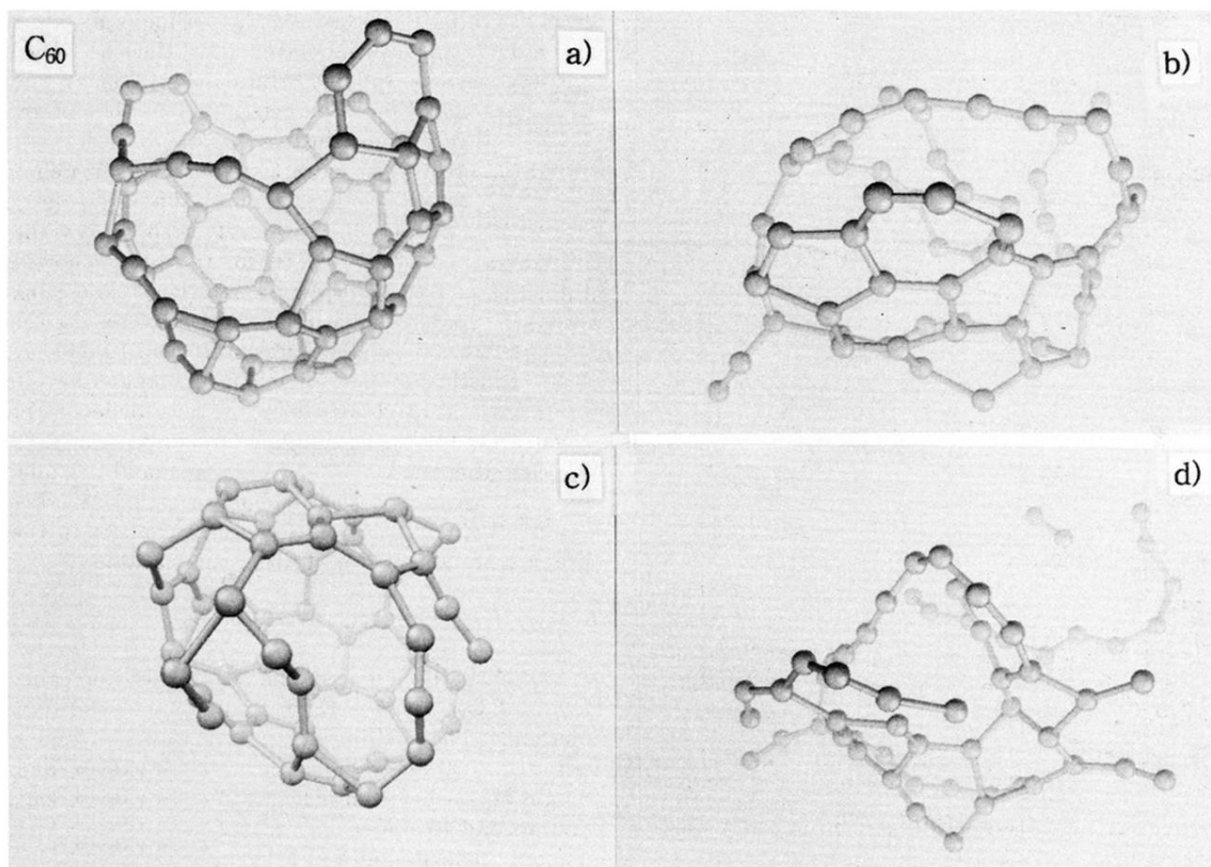


FIG. 4. Time evolution of snapshots of C₆₀ at 5000 K for every 500 time steps.

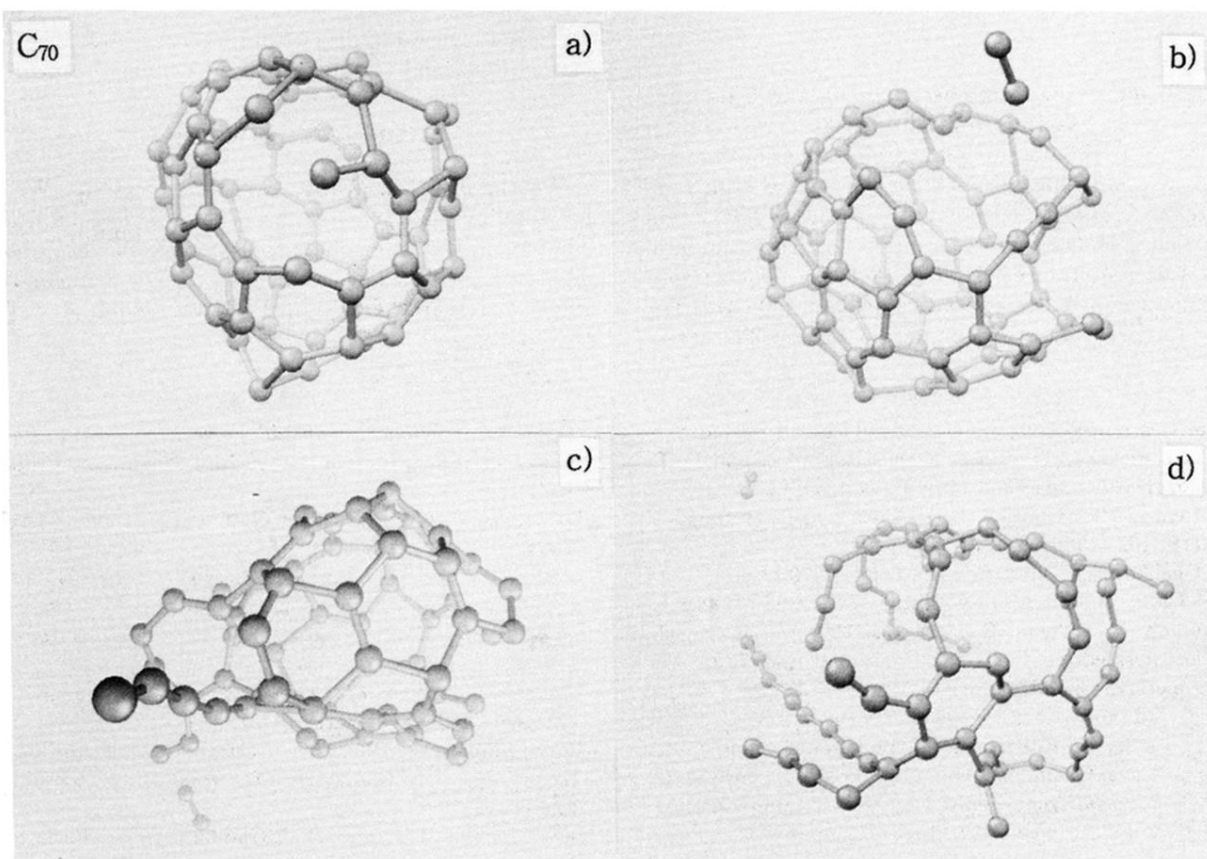


FIG. 5. Time evolution of snapshots of C_{70} at 5000 K for every 500 time steps.